Novel Algorithm for Real Time Imaging of Objects in a half-space with Unknown Characteristics

Yanli Liu[1,2], Lianlin Li[1], Fang Li [1]
[1]Institute of Electronics, Chinese Academy of Sciences, Beijing, China
[2]Graduate School of Chinese Academy of Sciences, Beijing, China
[1,2]ylliu04@mails.gucas.ac.cn

Introduction

During the past several decades, electromagnetic inverse scattering techniques grow more attractive. It has been widely used in several applications conducted with nondestructive tests and evaluations. The sensing of buried targets and landmines detection is an important branch of the inverse scattering. Since 1980's there has been a considerable research interest in the diffraction tomography methods for problems associated with subsurface characterization [1-3]. There also have been a lot of other methods to solve the half-space problems such as Distorted Born iterative method (DBIM) [4] and the method of MUltiple Signal Classification (MUSIC) [5] etc.

However the usual algorithms mentioned above require the characteristics of the half-space to be known. Relatively small errors in the estimated ε_b-value may result in large distortions of reconstructed profile. In this paper a novel auto-focusing approach has been proposed to the reconstruction of dielectric objects in a lossy earth with unknown characteristics. The fast Fourier transform has been used to cut down the computing time. An exponential refocusing time factor has been introduced. The rule to choose the optimal focusing time is determined by the minimum entropy criterion. Numerical results have shown that the proposed algorithm can provide a good location of the embedded objects in a short computing time despite the inaccurate estimation of earth electrical parameters.

Formulation

Fig.1 has shown the configuration of the 2-D half-space imaging problem. The upper region is a free space ($\varepsilon_a = 1, \sigma_a = 0$). The lower region is a lossy earth characterized by ε_b and σ_b. D_{obs} denotes the observation domain. The transceiver is located in a plane above or on the air-earth interface: $y = y_s \geq 0$ and parallel to the interface. (x_s, y_s) indicates the position of the transceiver and y_s is a constant here. The transceiver moves along a scan line ranging from $(-L/2, y_s)$ to $(L/2, y_s)$, which is parallel to the surface as shown in Fig.1.

Suppose that the electric current is a 2-D point source, which is equivalent to a 3-D line source directed to *z* direction. In this case only the *z* component of the electric field is nonzero and the subscript z will be omitted in the following formulations. Under Born approximation we have

$$E_{scat}(\boldsymbol{\rho}_s;k) = k^2 \int_{Dobs} G_{ab}(\boldsymbol{\rho}_s, \boldsymbol{\rho}';k) E_{inc}(\boldsymbol{\rho}';\boldsymbol{\rho}_s,k) \chi(\boldsymbol{\rho}') d\boldsymbol{\rho}' \quad (1)$$

Here we assume a frequency independency of the objects.

The incident electric field can be modeled as

$$E_{inc}(\boldsymbol{\rho}';\boldsymbol{\rho}_s,k) = ik\eta_0 P(k) G_{ab}(\boldsymbol{\rho}', \boldsymbol{\rho}_s;k) \quad (2)$$

Using reciprocity theorem $G_{ab}(\boldsymbol{\rho}', \boldsymbol{\rho}_s;k) = G_{ab}(\boldsymbol{\rho}_s, \boldsymbol{\rho}';k)$ and then applying the exploding-source model $G_{ab}(\boldsymbol{\rho}_s, \boldsymbol{\rho}';k) G_{ab}(\boldsymbol{\rho}_s, \boldsymbol{\rho}';k) = G_{ab}(\boldsymbol{\rho}_s, \boldsymbol{\rho}';2k)$ to Eq.(1) it becomes

978-1-4244-2642-3/08/$25.00 ©2008 IEEE

$$E_{scat}(\boldsymbol{\rho}_s;k) = i\eta_0 k^3 \int_{Dobs} d\boldsymbol{\rho}' G_{ab}(\boldsymbol{\rho}_s,\boldsymbol{\rho}';2k) P(k) \chi(\boldsymbol{\rho}')$$

(3)

Eq.(3) can be expressed in the form of an operator $A:\chi \to E_{scat}$ .By using the Weyl identity, the operator $\boldsymbol{A}$ can be expressed as

$$A(\square) \square -\frac{\eta_0 k^3}{2\pi} \int_{Dobs} \int_{-\infty}^{\infty} d\boldsymbol{\rho}' dk_x P(k) \frac{\exp\left\{i\left[k_x(x_s - x') + k_{ay} y_s - k_{by} y'\right]\right\}}{k_{ay} + k_{by}} (\square)$$

(4)

where $k_{ay,by} = \sqrt{4k^2 \varepsilon_{a,b} - k_x^2 + ik\eta_0 \sigma_{a,b}}$.

Then the buried dielectric cylinders can be reconstructed

$$\chi(\boldsymbol{\rho}') = A^{\mathrm{H}}\left[E_{scat}(\boldsymbol{\rho}_s;k)\right]$$

(5)

A^{H} is the adjoint operator of A . Then

$$\chi(\boldsymbol{\rho}') = -\frac{\eta_0}{2\pi} \int_{k_{\min}}^{k_{\max}} k^3 P^*(k) dk \int_{-\infty}^{\infty} dk_x \tilde{E}_{scat}(k_x;k) \frac{\exp\left[ik_x x' - ik_{ay}^* y_s + ik_{by}^* y'\right]}{k_{ay}^* + k_{by}^*}$$

(6)

By using FFT, Eq.(6) can be calculated in a short computation time. In Eq.(5) regularization of an ill-posed matrix has been avoided. Since the spectral form of Green's function has been adopted in Eq.(6) it can be applied to multi-layered case easily.

Auto-focusing Technique

In Eq.(6) the permittivity of the earth are needed. However sometimes there is no a priori exact information about the earth permittivity. Inspired by the concept of time reversal imaging (TRI), Eq.(6) can be interpreted as

$$\chi(\boldsymbol{\rho}',t)\big|_{t=0} = -\frac{\eta_0}{2\pi} \int_{k_{\min}}^{k_{\max}} k^3 P^*(k) dk \int_{-\infty}^{\infty} dk_x \tilde{E}_{scat}(k_x;k) \frac{\exp\left[ik_x x' - ik_{ay}^* y_s + ik_{by}^* y'\right]}{k_{ay}^* + k_{by}^*} \exp(j\omega t)\big|_{t=0}$$

(7)

If the permittivity of the earth is not estimated exactly the optimal focusing time will not be at $t = 0$. Thus the reconstruct formula of the object function can be modified into

$$\chi(\boldsymbol{\rho}',t) = -\frac{\eta_0}{2\pi} \int_{k_{\min}}^{k_{\max}} k^3 P^*(k) dk \int_{-\infty}^{\infty} dk_x \tilde{E}_{scat}(k_x;k) \frac{\exp\left[ik_x x' - ik_{ay}^* y_s + ik_{by}^* y'\right]}{k_{ay}^* + k_{by}^*} \exp(j\omega t)$$

(8)

According to Eq.(8) a series of images can be obtained with different *t* values. Employ the minimum entropy criterion [6] to determine the most optimal focusing time. The entropy of one image is defined as

$$e\left[\chi(\boldsymbol{\rho}')\right]\big|_t = \sum_{j=1}^{yN}\left[\sum_{i=1}^{xN}\left|\chi_{ij}\right|^2\right]^2 \Big/ \sum_{j=1}^{yN}\sum_{i=1}^{xN}\left|\chi_{ij}\right|^4$$

(9)

Minimizing the entropy the corresponding instant t_0 is the optimal focusing time. Reviewing the imaging process describe above we can find that the auto-focusing process is in a way

similar to time reversal which consists of two steps. First reverse the received signal in time domain. Second retransmit the reversed signals in the same medium. Likewise in the proposed auto-focusing algorithm if the optimal time is adopted the signals will be refocused at the true location of the target and vice versa.

Reconstruction Results

In the numerical simulations considered in this section, let $\varepsilon_b = 6,\ \sigma_b = 0.1\text{mS/m}$. The reconstruction domain D_{obs} is a 1m×1m square region whose top side is 0.5m below the air-soil interface. The height of transceivers is $y_s = 3\text{m}$ and $L = 10\text{m}$. There are 100 transceiver positions with a step of 0.1m. The working frequency is between 200MHz-1.2GHz with a step of 50MHz. The scattered data are simulated using CG-FFT algorithm.

First, we will see distortions in the reconstructed images caused by the errors in the estimated ε_b' and σ_b'-value. The prime represents the estimated value distinct from the true one. We consider a square dielectric object ($\varepsilon_r = 10, \sigma_r = 0.2\text{mS/m}$) of 4cm×4cm centered at (0,-1.02m).The original object profiles to be reconstructed are shown in Fig.2(a). Fig.2(b-d) show the images with different estimated values $\varepsilon_b' = 4, \sigma_b' = 5\text{mS/m}$, $\varepsilon_b' = 6, \sigma_b' = 0.1\text{mS/m}$, $\varepsilon_b' = 12, \sigma_b' = 5\text{mS/m}$ respectively. In Fig.2(b) and (d) there exists obvious position deflection and image blurring. Only Fig.2(c) achieves a satisfactory image with the exact values of ε_b and σ_b. Second, we explore the cause of the image degradation in the concept of TRI. Put the exact ε_b and σ_b values into Eq.(6). The degradation of the image caused by the inaccurate estimation of ε_b can be explained as the focusing time is unsuitable chosen in the sense of TRI, shown in Fig.3(a-c). Only at $t = 0$ we can obtain a satisfactory reconstructed image. If we choose another time $t \neq 0$ it will result in image degradation which is similar to the image position deflection caused by inaccurate estimation of ε_b' and σ_b'. Third, apply the auto-focusing technique to remove the degradation caused by the inaccurate estimation of ε_b' and σ_b'. Here $\varepsilon_b' = 10, \sigma_b' = 5\text{mS/m}$ is adopted. Fig.4(a) shows the result without auto-focusing. Fig.4 (b) shows the entropy curve. The optimal time t_0 can be easily extracted from Fig.4(b). Then we can get the final satisfactory image as shown in Fig.4(c) regardless of the estimation inaccuracy of ε_b' and σ_b'.

Discussion and Conclusions

From Fig.2 (b-d) we can see that the estimation error results in a distorted image in which the object is located in a wrong position. By employing auto-focusing technique the image distortion will be removed, which has been shown in Fig.4(c). Numerical results have displayed that the proposed algorithm can provide a good locations of the object embedded under a lossy earth despite the inaccurate estimation of earth electrical parameters in a very short computing time.

Acknowledgement: This work is supported by National Natural Science Foundation of China under Grant No.60701010 and No.40774093.

References

[1] A.J.Devaney, “Geophysical diffraction tomography,” *IEEE Trans.Geosci. Remote Sensing,* vol.GE-22, pp. 3-13, Jan.1984.

[2] R.Deming and A.J.Devaney, “Diffraction tomography for multi-monostatic ground penetrating radar imaging,” *Inverse. Problem.,* vol. 13, pp.29-45, 1997.

[3] Tie Jun Cui and Weng Cho Chew, “Diffraction tomographic algorithm for the detection of three-dimensional objects buried in a lossy half-sapce,” *IEEE Trans. Antennas Propagat.,* vol.50, no.1, 2002.

[4] Tie Jun Cui and Weng Cho Chew, “Inverse scattering of two-dimensional dielectric objects buried in a lossy earth using the distorted Born iterative method,” *IEEE Trans.Geosci. Remote Sensing,* vol.39, no.2, 2001.
[5] E.Iakovleva, S.Gdoura, D.Lesselier and G.Perrusson, “Multistatic response matrix of a 3-D inclusion in half space and MUSIC imaging,” *IEEE Trans. Antennas Propagat.,* vol.55, no.9, 2007..
[6] H.Wu, J.Barba, “Minimum entropy restoration of star field images,” *IEEE Trans. Systems,* Man and Cybernetics part B:Bybernetics, vol.28, no.2, pp:227-231,1998.

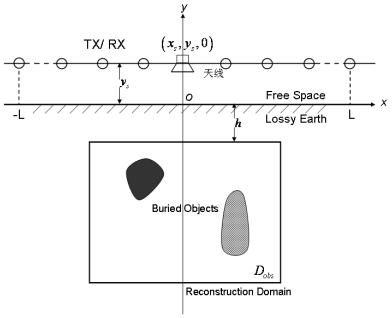

Fig.1 Physical configuration of half-space imaging problem

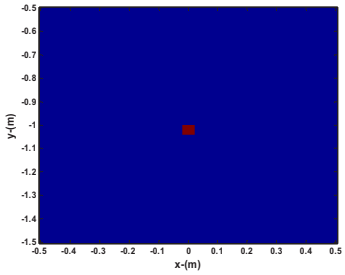

Fig.2 (a)

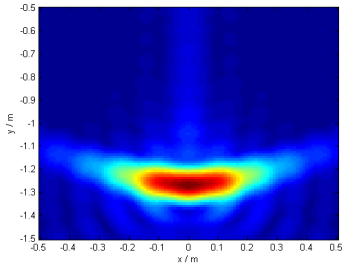

Fig.2 (b)

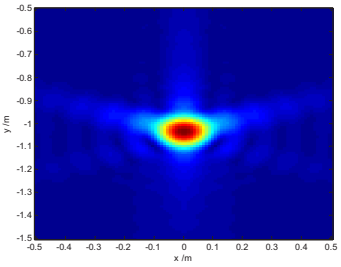

Fig.2(c)

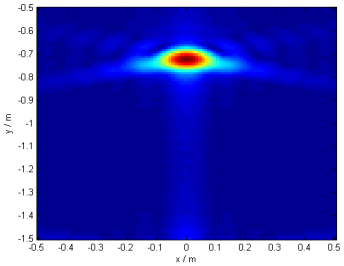

Fig.2(d)

Fig.2 reconstructed results with different estimated values ε_b' and σ_b' (no auto-focusing):(a) original profile(b) $\varepsilon_b' = 4, \sigma_b' = 5\text{mS/m}$, (c) $\varepsilon_b' = 6, \sigma_b' = 0.1\text{mS/m}$, (d) $\varepsilon_b' = 12, \sigma_b' = 5\text{mS/m}$

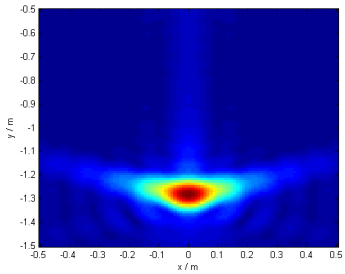

Fig.3 (a)

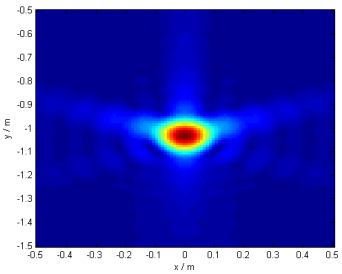

Fig.3(b)

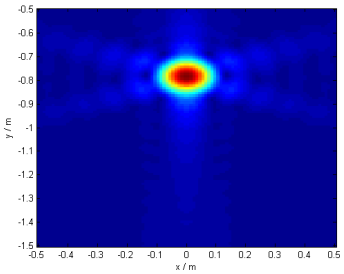

Fig.3(c)

Fig.3 imaging results with the exact parameters of earth $\varepsilon_b' = 6$ and $\sigma_b' = 0.1\text{m}S/\text{m}$ at different focusing time:(a) t=4ns, (b) t=0, (c) t=-4ns

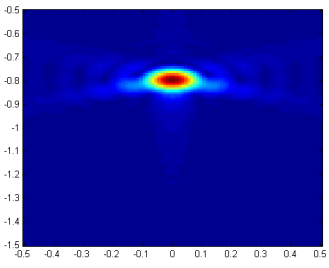

Fig.4 (a)

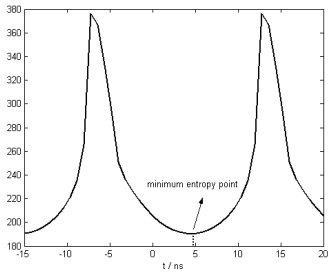

Fig.4 (b)

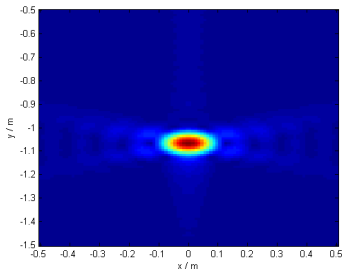

Fig.4 (c)

Fig.4 reconstructed results with $\varepsilon_b' = 10$ $\sigma_b' = 5\text{mS/m}$: (a) without auto-focusing(b) entropy curve (c) optimal image